


# Combination of Astragali Polysaccharide and Curcumin Improves the Morphological Structure of Tumor Vessels and Induces Tumor Vascular Normalization to Inhibit the Growth of Hepatocellular Carcinoma

Integrative Cancer Therapies  
Volume 18(1): 1–8  
© The Author(s) 2019  
Article reuse guidelines:  
sagepub.com/journals-permissions  
DOI: 10.1177/1534735418824408  
journals.sagepub.com/home/ict  


Decai Tang, MD<sup>1,\*</sup>, Shuo Zhang, MD<sup>2,\*</sup>, Xiaoxia Shi, MS<sup>1</sup>, Jiafei Wu, MBBS<sup>1</sup>, Gang Yin, MD<sup>1</sup>, Xiyang Tan, MPharma<sup>3</sup>, Fuyan Liu, MBBS<sup>1</sup>, Xingdong Wu, MBBS<sup>1</sup>, and Xiangyu Du, MBBS<sup>1</sup>

## Abstract

Normalizing the disordered tumor vasculature, rather than blocking it, is a novel method for anticancer therapy. Astragali polysaccharide (APS) and curcumin were reported to be active against carcinomas. However, the effect and mechanism of the combination of APS and curcumin on vascular normalization in hepatocellular carcinoma (HCC) was not clear. In the present study, effects of combined APS and curcumin on tumor vascular normalization were evaluated in HepG2 tumor-bearing mice. Photoacoustic tomography (PAT) was performed to observe the morphological structure of tumor vessels *in vivo*. The microstructure of the tumor vessels was also analyzed through scanning electron microscopy. Additionally, the expression of CD31 and NG2 was analyzed by immunohistochemical staining. Tumor vessels of HepG2 tumor-bearing mice treated with the combination were sparse with uniform growth, morphology rules, and complete vascular walls, which had fewer branches and sprouts. ECs of tumor vessels were arranged regularly and were tightly connected, tending toward normalization. The expression of CD31 was reduced while NG2 was increased significantly by the combination of APS and curcumin. The results indicated that APS and curcumin in combination showed a better effect on inhibiting tumor growth in an orthotopic nude-mouse model of HCC. More important, the combination induced normalization of tumor vascular better than APS or curcumin administration alone, improving the morphological structure of tumor vessels and promoting maturation of tumor vessels. The results of the present study provided a reasonable possibility for combination therapy of APS and curcumin in the treatment of HCC via tumor vascular normalization.

## Keywords

vascular normalization, photoacoustic tomography, Astragali polysaccharide, curcumin, hepatocellular carcinoma

Submitted August 21, 2018; revised November 30, 2018; accepted December 13, 2018

## Introduction

Hepatocellular carcinoma (HCC) has been regarded as one of the most common malignancies responsible for cancer-associated mortality.<sup>1</sup> The common clinical therapies, such as radiotherapy and chemotherapy, are not ideal due to the toxic side effects and easily induced tumor resistance. Angiogenesis is a crucial process in the development of

solid tumors, comprising proliferation, invasion, and dissemination.<sup>2</sup> Most antiangiogenic methods aim to block angiogenesis, reduce blood supply to tumor tissue, and limit the supply of oxygen and nutrients to starve tumor cells.<sup>3</sup> However, antiangiogenic drugs have not absolutely fulfilled expectations in the clinical setting, especially due to tumors developing resistance and evasion mechanisms.



As we know, tumor angiogenesis is accompanied by vasculogenesis. Essentially, tumor vessels are tortuous, with uneven diameters and irregular branching patterns. The vascular wall is thin with many cracks. Endothelial cells (ECs) of vessels detach from the basement membrane resulting in separation from each other. The structural abnormalities of tumor vessels, along with ECs that are loosely connected and reduced coverage of pericytes, account for the reduced efficacy of anticancer treatments. So normalizing the disordered tumor vasculature, rather than blocking it, is a novel method for anticancer therapy.<sup>4</sup> Traditional Chinese herbal drugs, especially the active compositions such as sinomenine hydrochloride, display antiangiogenic effects and enhance tumor vascular normalization.<sup>5-7</sup>

Our previous study revealed that *Astragalus membranaceus* and *Curcuma wenyujin* in combination has a remarkable effect on inhibiting different stages of ovarian cancer progression<sup>8</sup>; thus, we have focused on the effect of the drug pair *Astragalus membranaceus* and *Curcuma wenyujin* on cancer progression a long time. Astragali polysaccharide (APS) is the primary active constituent of *Astragalus membranaceus*, and curcumin is a major component of *Curcuma wenyujin*. Both of them have been reported to possess antitumor effects.<sup>9-17</sup> However, the synergistic effect of APS and curcumin in combination on monitoring tumor angiogenesis and tumor growth in HCC was unclear.

In the present study, we aimed to evaluate the feasibility of the combination of APS and curcumin by noninvasively monitoring tumor angiogenesis in the HCC orthotopic mouse model, providing experimental evidence for clinical application.

## Materials and Methods

### Cell Culture

The HepG2 human hepatocarcinoma cell line was purchased from EnoGene (Nanjing, China). Cells were cultured in RPMI-1640 medium (Gibco, Grand Island, NY) with 10% fetal bovine serum (Gibco) plus 1% penicillin and streptomycin in a 5% CO<sub>2</sub> atmosphere at 37°C. Cells in the

logarithmic period were used for subsequent experiments, and the medium was renewed every other day.

### Orthotopic Xenograft Model

Male BALB/c nude mice (18-20 g) of 4 to 5 weeks age were provided by CAVENS Animal Co, Ltd (Changzhou, China). Briefly, mice were maintained under standard environmental conditions with temperature of 25 ± 1°C, relative humidity of 50 ± 5%. Mice were fed with a standard diet and water ad libitum. After 7 days adaptation, 0.2 mL HepG2 cells (2.5 × 10<sup>7</sup>/mL) were injected into the flank of the nude mice. The tumors were removed after 14 days, and cut into 1 mm<sup>3</sup> pieces to transplant into the right lobe of the liver of nude mice to establish orthotopic xenograft models as previously described.<sup>18</sup> Animal performance was carried out in strict accordance with the recommendations in the *Guide for the Care and Use of Laboratory Animals* of the National Institutes of Health.

### Treatment

After the third day of orthotopic tumor implantation, mice were randomly divided into 4 groups (6 mice/group): the vehicle group (gavage of 0.01 mL/g normal saline); the APS group (gavage of 100 mg/kg APS); the curcumin group (gavage of 100 mg/kg curcumin); and the combination group (gavage of 100 mg/kg APS and 100 mg/kg curcumin). Animals were treated daily for 21 days.

### Photoacoustic Tomography

The Nexus 128 (Endra Inc, Ann Arbor, MI) photoacoustic tomography (PAT) system was used to monitor vasculature change in the orthotopic liver cancer model. At the end of administration, animals were anesthetized using a mixture of isoflurane and air, with levels adjusted to maintain a respiration rate of 100 breaths per minute. The tumor was located at the center of the notch in the tray, and the tumor tissue was immersed in pure water to provide acoustic coupling. The tray was placed in the scanning room of the PAT system, making sure the tray was located on the upper slot. Imaging

<sup>1</sup>School of Nanjing University of Chinese Medicine, Nanjing, Jiangsu, People's Republic of China

<sup>2</sup>Nantong Hospital of Traditional Chinese Medicine, Nantong Affiliated Hospital of Nanjing University of Chinese Medicine, Nantong, Jiangsu, People's Republic of China

<sup>3</sup>Jiangsu Province Hospital of Traditional Chinese Medicine, Affiliated Hospital of Nanjing University of Chinese Medicine, Nanjing, Jiangsu, People's Republic of China

\*These two authors contributed equally to this work.

### Corresponding Author:

Decai Tang, Department of Chinese Medicine, Nanjing University of Chinese Medicine, 138 Xianlin Road, Nanjing, Jiangsu 210023, People's Republic of China.

Email: talknow@163.com

was performed with scans acquired at wavelengths of 680 nm using a continuous rotation (120 angles, 15 pulses).

### Scanning Electron Microscopy

Mice in the 4 groups were sacrificed following PAT. Tumor tissues were removed and weighed. The tissues were broken into small pieces and placed in 3% glutaraldehyde (Aladdin, Shanghai, China) to fix. Each sample was then washed with 0.1 M phosphate buffer solution (pH 7.2) 3 times for 1 hour and dehydrated in 30%, 50%, 70%, 90%, and 100% ethanol for 15 minutes each time. Samples were subsequently dried using the critical drying method. The vascular morphology was directly observed under a Quanta 200 scanning electron microscope (FEI, Hillsboro, OR).

### Immunohistochemistry

The tumor tissues were deparaffinized in xylene and rehydrated in a series of graded alcohols. Antigen was retrieved in 0.01 M sodium citrate buffer. Samples were incubated with 3% H<sub>2</sub>O<sub>2</sub> for 10 minutes and then blocked in 1% bovine serum albumin for 15 minutes. The slides were incubated with primary antibodies: cluster of differentiation 31 (CD31; 1:200, CST, MA) and neural/glial antigen 2 (NG2; 1:200, Abcam, Cambridge, UK) at 37°C for 2 hours. The secondary antibody labeled by horseradish peroxidase was followed added at 37°C for 20 minutes. The sections were counterstained with Mayer's hematoxylin. Using Image-Pro Plus 6.0 software (Media Cybernetics, Bethesda, MD) for gray value analysis, each slice was made up of 5 views and calculated the average.

### Statistical Analysis

All data were expressed as means  $\pm$  standard deviation. Statistical analysis was performed by 1-way analysis of variance based on Student's 2-tailed unpaired *t* test or Dunnett's multiple comparisons test using GraphPad Prism 5.0 software (GraphPad Software, San Diego, CA). Image-Pro Plus software 6.0 (Media Cybernetics, Inc, Silver Spring, MD) was used for processing images. A value of  $P < .05$  was considered to be a statistically significant difference for all tests.

## Results

### Combination of APS and Curcumin Improved the General Condition of Nude Mice

Twelve days after administration, the behavior of nude mice in the vehicle group was abnormal, with reduced activity and food intake as well as diarrhea. The behavior in the APS and curcumin combination group was normal, with rapid

movements and normal food intake without vomiting or diarrhea. The results showed that the combination of APS and curcumin can improve the behavioral state, appetite, and gastrointestinal reactions of nude mice.

### Combination of APS and Curcumin Inhibited Tumor Growth In Vivo

To evaluate the effects of APS and curcumin on tumor growth, the HCC orthotopic mouse model was established. Tumor weight was significantly reduced by combination of APS and curcumin compared with the vehicle control ( $P < .05$ ; Figure 1). The tumor inhibition of APS, curcumin, and combination group was 11.2%, 17.8%, and 49.8%, respectively.

### Combination of APS and Curcumin Improved the Morphological Structure of Tumor Vessels

PAT was used to investigate whether the morphological structure of tumor vessels was modified by combination of APS and curcumin treatment. In the absence of any exogenous contrast agent, PAT could clearly identify tumor neovascularization (Figure 2A). Tumor vessels in the vehicle, APS, and curcumin alone groups were abundant and tortuous, branched chaotically, and had uneven vessel lumens, revealing the heterogeneity of tumor vessels. However, vessels in the combination treatment group were less irregular, less tortuous, and had fewer branches and sprouts. The mice of APS and curcumin alone groups showed no significant decrease in branches and areas of the vessels compared with that in the vehicle group. Interestingly, mice in the combination group showed a significantly greater decrease in branches and areas of the vessels than that of the APS or curcumin alone groups ( $P < .01$ ), indicating synergistic efficacy on improvement the morphological structure of tumor vessels by combination of APS and curcumin treatment (Figure 2B and C).

The microstructure of the tumor vessels was also analyzed through scanning electron microscopy. It was observed that tumor vessels in the vehicle, APS, and curcumin alone groups exhibited marked abnormalities, with an abundant array of tortuous irregular distorted vessels, and an incomplete vascular wall. The tumor vascular morphology tended toward normalization after the treatment with combination of APS and curcumin (Figure 2D).

### Combination of APS and Curcumin Improved the Connection of ECs and Tumor Vessel Maturation

The connection of ECs was assessed on the basis of immunohistochemistry with antibodies against platelet EC adhesion

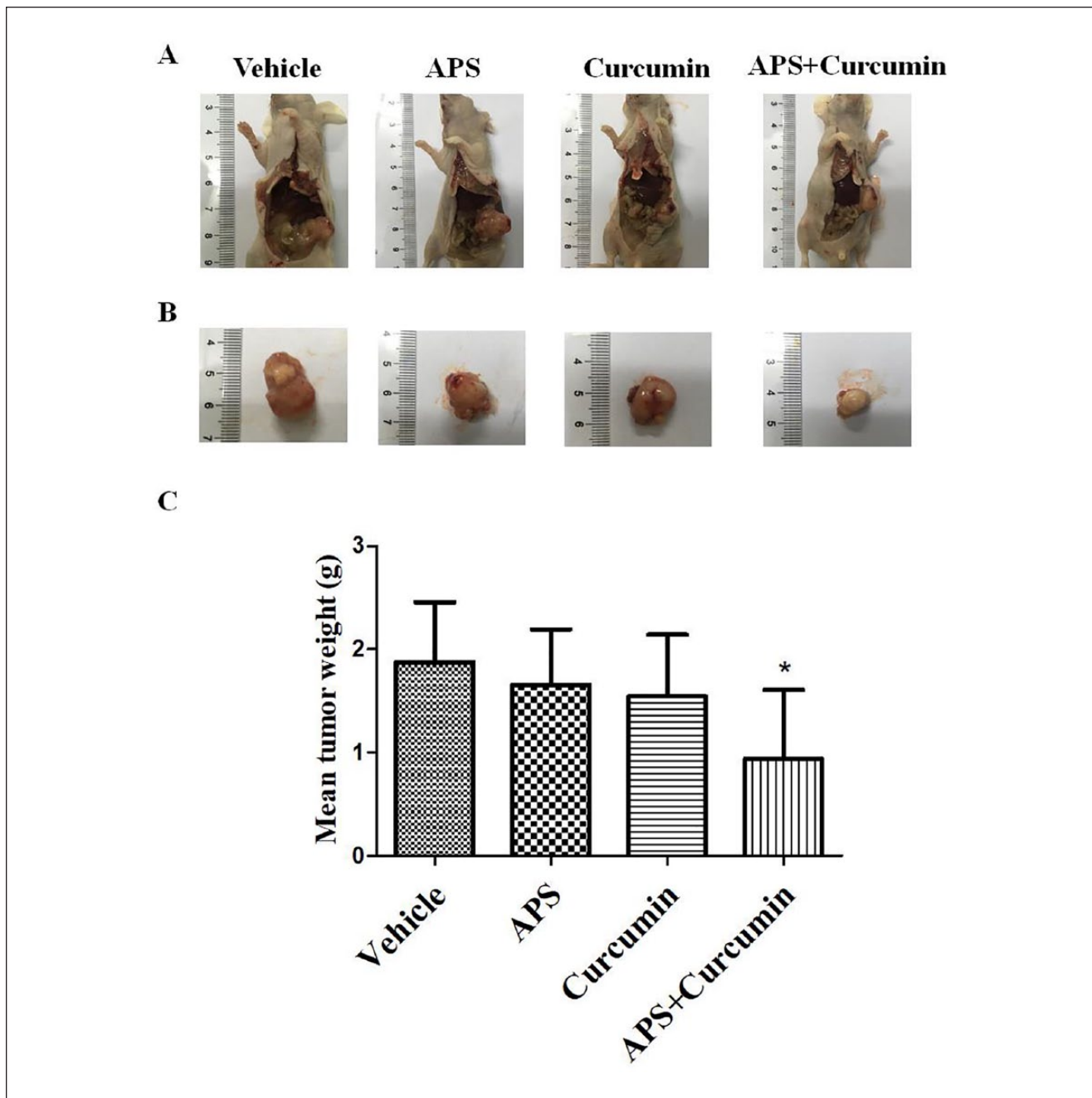


**Figure 1.** Efficacy of combination of Astragali polysaccharide (APS) and curcumin on tumor growth in the hepatocellular carcinoma (HCC) orthotopic nude-mouse model. (A) Representative orthotopic liver tumors of each treated group at autopsy; (B) representative excised liver tumors of each treated group at autopsy; and (C) mean tumor weight of each treated group. Results are presented as the mean  $\pm$  SD ( $n = 6$ ). \* $P < .05$  versus vehicle control.

molecule-1 (CD31/PECAM-1), an adhesion molecule on the surface of ECs. Compared with the vehicle group, ECs of tumor vessels in the APS-curcumin combination group were arranged regularly and were tightly connected. Compared with the vehicle, APS, or curcumin alone groups, administration with the APS-curcumin

combination significantly decreased the expression of CD31 ( $P < .01$ ), revealing the antiangiogenic effect (Figure 3A and B). However, compared with that in the vehicle group, HCC mice treatment with APS and curcumin alone showed no significant decrease in the expression of CD31.

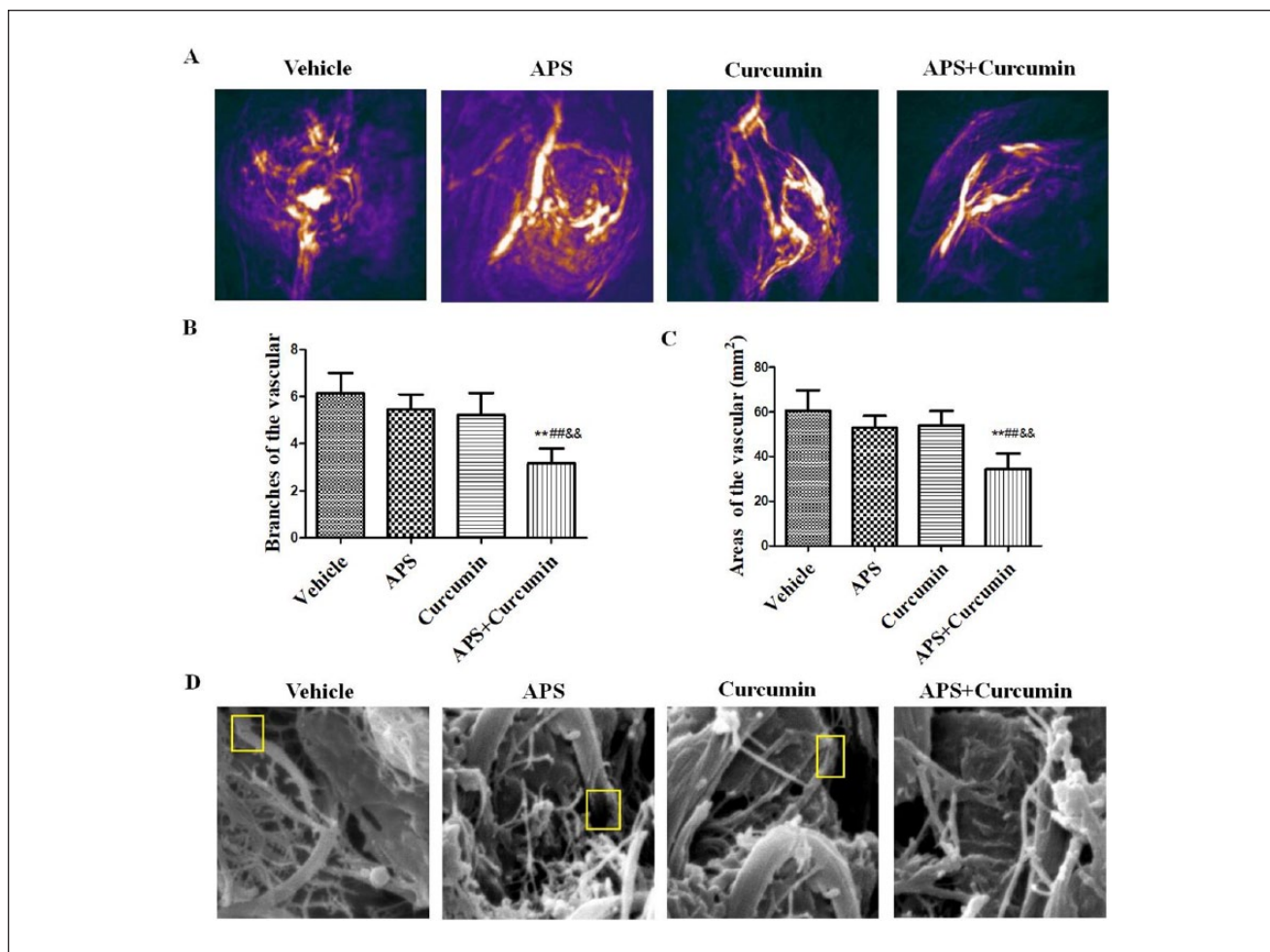


**Figure 2.** Efficacy of combination of APS and curcumin on the morphological structure of tumor vessels. (A) Representative morphological structure of tumor vessels observed by photoacoustic tomography (PAT) at wavelengths of 680 nm; (B) vascular branches of each treated group; (C) vascular areas of each treated group; and (D) representative microstructure of the tumor vessels detected by scanning electron microscopy. Scale bar, 5  $\mu\text{m}$ . Results are presented as the mean  $\pm$  SD. \*\* $P < .01$  versus vehicle control; ### $P < .01$  versus APS group; && $P < .01$  versus curcumin group.

Immature angiogenesis has been shown to lack pericyte coverage. Therefore, we further analyzed the effects of combination of APS and curcumin on pericytes in tumor vessels by studying the presence of NG2 proteoglycan, a specific pericyte marker. We observed that the expression of NG2 in tumors of all treatment groups was significantly upregulated compared with those of the vehicle control ( $P < .01$ ). The highest NG2 expression was found in the APS-curcumin combination group compared with the APS- and curcumin-treated groups ( $P < .01$ ), indicating synergistic effect of APS and curcumin on promoting maturation of tumor vessels (Figure 3C and D).

## Discussion

The abnormalities in ECs, basement membrane, and cell junctions collectively conduce to excessively leaky tumor

vessels.<sup>19</sup> And the tumor microenvironment with hypoxia and acidosis induced by tumor vascular leakage potentially reduce the efficacy of anticancer treatments. The theory of “tumor vascular normalization” proposed implies pruning the immature tumor vasculature, leading to vascular remodeling toward a normal vasculature.<sup>20</sup> Rectification of the structure of tumor vasculature would ultimately contribute to improving drug delivery for cancer treatment.

We initially evaluated the effects of APS and curcumin on tumor growth in an orthotopic nude-mouse model of HCC. The result showed that tumor weight was significantly reduced by combination of APS and curcumin, revealing an inhibitory effect on tumor growth, raising the question of the specific antitumor mechanism. We then investigated the efficacy of APS and curcumin on tumor vascular normalization, specifically including morphological structure and maturation of tumor vessels.

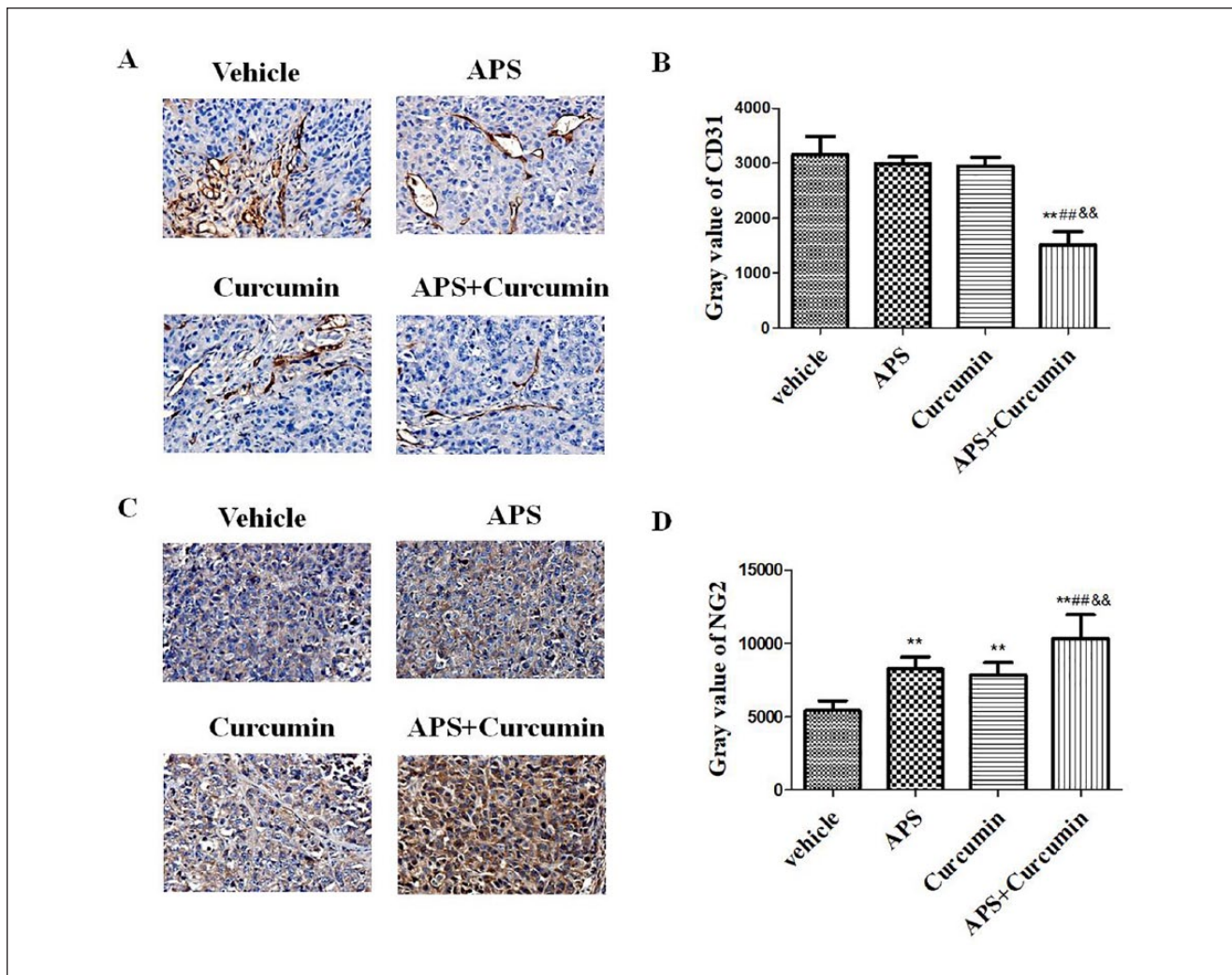


**Figure 3.** Efficacy of combination of APS and curcumin on the expression of CD31 and NG2. (A) Representative immunohistochemical staining for CD31 in the tumor at  $\times 20$  magnification; (B) gray value of CD31; (C) representative immunohistochemical staining for NG2 in the tumor at  $\times 20$  magnification; and (D) gray value of NG2. Results are presented as the mean  $\pm$  SD.  $**P < .01$  versus vehicle control;  $###P < .01$  versus APS group;  $\&\&P < .01$  versus curcumin group.

Traditional imaging techniques are frequently limited by narrow penetration, low sensitivity, low specificity, and poor spatial resolution. Hybrid modalities such as PAT, an emerging molecular imaging modality, have greatly contributed to improving most of these limitations. In particular, the imaging depth of the Nexus 128 PAT system attains 20 mm below the epidermis. Hence, the vascular structure around the tumor in vivo is imaged clearly by Nexus 128 PAT system due to the high resolution of 280  $\mu\text{m}$ . The Nexus 128 PAT system has been used to monitor the photoacoustic image of angiography in an orthotopic murine gastric carcinoma model.<sup>21</sup> Hence, we performed PAT to monitor tumor angiogenesis by combination of APS and curcumin treatment, to further provide images of the tumor vasculature in vivo, and to reveal the morphological feature

of vessels. There were more sparse blood vessel networks, homogeneous vessel distribution, and a significantly greater decrease in branches and areas of the vessels in mice of APS-curcumin combination group than in the vehicle, APS, or curcumin alone groups. The result indicated that combination of APS and curcumin improved the morphological structure of tumor vessels. PAT can potentially become a powerful tool for tumor diagnosis and treatment monitoring both in cancer research and clinical.

It is reported that direct restoration of vascular junctions and preservation of the vascular integrity could be a significant strategy to induce normalization of tumor blood vessels and reduce metastasis.<sup>22</sup> The microstructure of the tumor vessels was analyzed through scanning electron microscopy. The result showed that irregular distorted

vessels and an incomplete vascular wall was observed in vehicle, APS, and curcumin alone groups, while the tumor vascular morphology tended toward normalization with marked changes after the administration of APS-curcumin. The 2 angiographic techniques confirmed that combination of APS and curcumin showed a synergistic effect on improving morphological structure of tumor vessels and inducing normalization of tumor vascular.

The tumor cells and ECs interacted morphologically via pseudopodia and used alternative pathways to generate new vessels.<sup>23</sup> Platelet EC adhesion molecule-1 also known as CD31, an adhesion molecule on the surface of ECs, makes up a large portion of EC intercellular junctions.<sup>24</sup> CD31 is seen as an EC marker and is involved in leukocyte transmigration, angiogenesis, and integrin activation.<sup>25</sup> The adenocarcinoma cells and tumor tissue section became strongly positive for CD31.<sup>26-28</sup> In addition, we explored the combination of APS and curcumin on the connection of ECs by CD31 staining. The result suggested that ECs of tumor vessels in the APS-curcumin combination group were arranged regularly and were tightly connected compared with those of the vehicle group. Moreover, the expression of CD31 was significantly decreased by the treatment of the APS-curcumin combination in HCC tissues, while there was no significant difference observed in HCC tissues of APS or curcumin alone administration.

Pericytes, an integral component of mature blood vessels, contribute to vascular quiescence and integrity.<sup>29</sup> Compared with normal tissue, the density of tumor-associated pericytes is not only low on vessels, but tumor pericytes also display abnormal morphology.<sup>30</sup> Clinical data have previously shown that the low pericyte coverage in vasculature is correlated with decreased patient survival.<sup>31</sup> NG2 is a typical marker for vessel-surrounding pericytes, which contribute to the stabilization of microvessels, the regulation of capillary blood flow, and angiogenesis.<sup>32</sup> In pericytes, NG2 expression is important for pericyte localization to endothelial layer and interaction with ECs.<sup>33</sup> In the present study, we further analyzed the effects of APS-curcumin combination on pericytes in tumor blood vessels by detecting the presence of NG2 proteoglycan. The highest NG2 expression was found in the APS-curcumin combination group compared with the APS- and curcumin-treated groups, indicating synergistic effect of APS and curcumin on promoting maturation of tumor vessels.

In conclusion, the present study suggested that APS and curcumin in combination inhibited tumor growth in an orthotopic nude-mouse model of HCC. Besides, combination of APS and curcumin induced normalization of tumor vascular, which comprised the improvement of morphological structure of tumor vessels and the promotion of maturation of tumor vessels. The results of the present study provided a reasonable possibility for the

combination therapy of APS and curcumin for the treatment of HCC via tumor vascular normalization, and may bring about a breakthrough for an effective anticancer therapy. Based on the results and the drug action characteristics of APS and curcumin, we will focus on the relevant possible immunity-associated mechanism in the near future.

### Acknowledgments

We thank all our colleagues in our research group for their generous support.

### Declaration of Conflicting Interests

The author(s) declared no potential conflicts of interest with respect to the research, authorship, and/or publication of this article.

### Funding

The author(s) disclosed receipt of the following financial support for the research, authorship, and/or publication of this article: The study was supported by the National Natural Science Foundation of China (No. 81373990).

### References

1. Lazarev S, Hardy-Abeloos C, Factor O, Rosenzweig K, Buckstein M. Stereotactic body radiation therapy for centrally located hepatocellular carcinoma: outcomes and toxicities. *J Cancer Res Clin Oncol*. 2018;144:2077-2083.
2. Kurmyshkina OV, Belova LL, Kovchur PI, Volkova TO. Remodeling of angiogenesis and lymphangiogenesis in cervical cancer development. *Biochem Suppl*. 2016;10:191-211.
3. Bhatia SK. Translation of pro-angiogenic and anti-angiogenic therapies into clinical use. In: Reinhart-King CA, ed. *Mechanical and Chemical Signaling in Angiogenesis*. Berlin, Heidelberg: Springer; 2013:261-278.
4. Gilles ME, Maione F, Cossutta M, et al. Nucleolin targeting impairs the progression of pancreatic cancer and promotes the normalization of tumor vasculature. *Cancer Res*. 2016;76:7181-7193.
5. Zhang H, Ren Y, Tang X, et al. Vascular normalization induced by sinomenine hydrochloride results in suppressed mammary tumor growth and metastasis. *Sci Rep*. 2015;5:8888.
6. Yang X, Wu XZ. Main anti-tumor angiogenesis agents isolated from Chinese herbal medicines. *Mini Rev Med Chem*. 2015;15:1011-1023.
7. Zhu WJ, Yu DH, Zhao M, et al. Antiangiogenic triterpenes isolated from Chinese herbal medicine *Actinidia chinensis* Planch. *Anticancer Agents Med Chem*. 2013;13:195-198.
8. Yin G, Tang D, Dai J, et al. Combination efficacy of *Astragalus membranaceus* and *Curcuma wenyujin* at different stages of tumor progression in an imageable orthotopic nude mouse model of metastatic human ovarian cancer expressing red fluorescent protein. *Anticancer Res*. 2015;35:3193-3207.
9. Zhou Z, Meng M, Ni H. Chemosensitizing effect of *Astragalus polysaccharides* on nasopharyngeal carcinoma cells by inducing apoptosis and modulating expression of Bax/Bcl-2 ratio and caspases. *Med Sci Monit*. 2017;23:462-469.

10. Xiang J, Xiang Y, Lin S, et al. Anticancer effects of deproteinized asparagus polysaccharide on hepatocellular carcinoma in vitro and in vivo. *Tumour Biol.* 2014;35:3517-3524.
11. Bao H, Liu P, Jiang K, et al. Huaier polysaccharide induces apoptosis in hepatocellular carcinoma cells through p38 MAPK. *Oncol Lett.* 2016;12:1058-1066.
12. Huang WH, Liao WR, Sun RX. Astragalus polysaccharide induces the apoptosis of human hepatocellular carcinoma cells by decreasing the expression of Notch1. *Int J Mol Med.* 2016;38:551-557.
13. Yang B, Xiao B, Sun T. Antitumor and immunomodulatory activity of Astragalus membranaceus polysaccharides in H22 tumor-bearing mice. *Int J Biol Macromol.* 2013;62:287-290.
14. Wang XP, Wang QX, Lin HP, Chang N. Anti-tumor bioactivities of curcumin on mice loaded with gastric carcinoma. *Food Funct.* 2017;8:3319-3326.
15. Darvesh AS, Aggarwal BB, Bishayee A. Curcumin and liver cancer: a review. *Curr Pharm Biotechnol.* 2012;13:218-228.
16. Tsai CF, Hsieh TH1, Lee JN, et al. Curcumin suppresses phthalate-induced metastasis and the proportion of cancer stem cell (CSC)-like cells via the inhibition of AhR/ERK/SK1 signaling in hepatocellular carcinoma. *J Agric Food Chem.* 2015;63:10388-10398.
17. Zeng Y, Shen Z, Gu W, Wu M. Inhibition of hepatocellular carcinoma tumorigenesis by curcumin may be associated with CDKN1A and CTGF. *Gene.* 2018;651:183-193.
18. Zhang S, Tang D, Zang W, et al. Synergistic inhibitory effect of traditional Chinese medicine astragaloside IV and curcumin on tumor growth and angiogenesis in an orthotopic nude-mouse model of human hepatocellular carcinoma. *Anticancer Res.* 2017;37:465-473.
19. Carmeliet P, Jain RK. Principles and mechanisms of vessel normalization for cancer and other angiogenic diseases. *Nat Rev Drug Discov.* 2011;10:417-427.
20. Jain RK. Normalization of tumor vasculature: an emerging concept in antiangiogenic therapy. *Science.* 2005;307:58-62.
21. Bao CC, Conde J, Pan F, et al. Gold nanoprisms as a hybrid in vivo cancer theranostic platform for in situ photoacoustic imaging, angiography, and localized hyperthermia. *Nano Res.* 2016;9:1043-1056.
22. Agrawal V, Maharjan S, Kim K, et al. Direct endothelial junction restoration results in significant tumor vascular normalization and metastasis inhibition in mice. *Oncotarget.* 2014;5:2761-2777.
23. Kaessmeyer S, Bhoola K, Baltic S, Thompson P, Plendl J. Lung cancer neovascularisation: cellular and molecular interaction between endothelial and lung cancer cells. *Immunobiology.* 2014;219:308-314.
24. Lee S, Valmikinathan CM, Byun J, et al. Enhanced therapeutic neovascularization by CD31-expressing cells and embryonic stem cell-derived endothelial cells engineered with chitosan hydrogel containing VEGF-releasing microtubes. *Biomaterials.* 2015;63:158-167.
25. Yoon JW, Jang IH, Heo SC, et al. Isolation of foreign material-free endothelial progenitor cells using CD31 aptamer and therapeutic application for ischemic injury. *PLoS One.* 2015;10:e0131785.
26. Xiao CX, Wang HH, Shi Y, et al. Distribution of bone-marrow-derived endothelial and immune cells in a murine colitis-associated colorectal cancer model. *PLoS One.* 2013;8:e73666.
27. Smeda M, Kieronska A, Adamski MG, et al. Nitric oxide deficiency and endothelial-mesenchymal transition of pulmonary endothelium in the progression of 4T1 metastatic breast cancer in mice. *Breast Cancer Res.* 2018;20:86.
28. Liang Y, Zhuo Y, Lin Z, et al. Decreased expression of MYPT1 contributes to tumor angiogenesis and poor patient prognosis in human prostate cancer. *Curr Mol Med.* 2018;18:100-108.
29. Xian X, Håkansson J, Ståhlberg A, et al. Pericytes limit tumor cell metastasis. *J Clin Invest.* 2006;116:642-651.
30. Bergers G, Song S. The role of pericytes in blood-vessel formation and maintenance. *Neuro Oncol.* 2005;7:452-464.
31. Cooke VG, LeBleu VS, Keskin D, et al. Pericyte depletion results in hypoxia-associated epithelial-to-mesenchymal transition and metastasis mediated by met signaling pathway. *Cancer Cell.* 2012;21:66-81.
32. Trost A, Lange S, Schroedl F, et al. Brain and retinal pericytes: origin, function and role. *Front Cell Neurosci.* 2016;10:20.
33. Ozerdem U, Stallcup WB. Pathological angiogenesis is reduced by targeting pericytes via the NG2 proteoglycan. *Angiogenesis.* 2004;7:269-276.